NIH Public Access
Author Manuscript
Cell Cycle. Author manuscript; available in PMC 2009 February 2.

Published in final edited form as:
Cell Cycle. 2008 October ; 7(19): 3062–3073.

Microarray and pathway analysis reveals decreased *CDC25A* and increased *CDC42* associated with slow growth of *BCL2* overexpressing immortalized breast cell line

Jacquelyn M. Long[1], **Charles W. Bell**[1], **W. Samuel Fagg IV**[1], **Mary E. Kushman**[2], **Kevin G. Becker**[3], **James A. McCubrey**[4], and **Mary A. Farwell**[1,*]

1*Department of Biology; East Carolina University; Greenville, North Carolina USA*

2*University of Pennsylvania Department of Pharmacology and Center of Excellence in Environmental Toxicology; 135 John Morgan Bldg; 3620 Hamilton Walk; Philadelphia, Pennsylvania USA*

3*Gene Expression and Genomics Unit; Research Resources Branch; National Institute on Aging; NIH; Baltimore, Maryland USA*

4*Department of Microbiology and Immunology; Brody School of Medicine; East Carolina University; Greenville, North Carolina USA*

Abstract

Bcl-2 is an anti-apoptotic protein that is frequently overex-pressed in cancer cells but its role in carcinogenesis is not clear. We are interested in how Bcl-2 expression affects non-cancerous breast cells and its role in the cell cycle. We prepared an MCF10A breast epithelial cell line that stably overexpressed *Bcl-2*. We analyzed the cells by flow cytometry after synchronization, and used cDNA microarrays with quantitative reverse-transcription PCR (qRTPCR) to determine differences in gene expression. The microarray data was subjected to two pathway analysis tools, parametric analysis of gene set enrichment (PAGE) and ingenuity pathway analysis (IPA), and western analysis was carried out to determine the correlation between mRNA and protein levels. The MCF10A/Bcl-2 cells exhibited a slow-growth phenotype compared to control MCF10A/Neo cells that we attributed to a slowing of the G_1-S cell cycle transition. A total of 363 genes were differentially expressed by at least two-fold, 307 upregulated and 56 downregulated. PAGE identified 22 significantly changed gene sets. The highest ranked network of genes identified by IPA contained 24 genes. Genes that were chosen for further analysis were confirmed by qRT-PCR, however, the western analysis did not always confirm differential expression of the proteins. Downregulation of the phosphatase *CDC25A* could solely be responsible for the slow growth pheno-type in MCF10A/Bcl-2 cells. Increased levels of GTPase Cdc42 could be adding to this effect. PAGE and IPA are valuable tools for microarray analysis, but protein expression results do not always follow mRNA expression results.

Keywords

Bcl-2; MCF10A; colchicine; microarray; qRT-PCR; PAGE; IPA

*Correspondence to: Mary A. Farwell; Biology Department; East Carolina University; Greenville, North Carolina 27858 USA; Email: farwellm@ecu.edu

NIH-PA Author Manuscript
NIH-PA Author Manuscript
NIH-PA Author Manuscript

NIH-PA Author Manuscript

NIH-PA Author Manuscript

NIH-PA Author Manuscript

Introduction

The B-cell lymphoma gene (*Bcl-2*) is a negative regulator of apoptosis, and its overexpression has been found in a large number of cancers.[1] Bcl-2 has been hypothesized to play two separate roles in the development and progression of cancer. First, the inhibition of apoptosis by Bcl-2 may allow cells to persist until other oncogenes such as *c-MYC* are activated.[2] In addition, Bcl-2 is a potent suppressor of apoptosis induced by most stress applications, including chemotherapeutic drugs.[3] Most anti-cancer agents are designed to induce apoptosis, yet overexpression of Bcl-2 increases drug resistance in cancer cells. Interestingly, although *Bcl-2* is over-expressed in breast cancer, its expression is associated with a positive prognosis.[4] This fact may be a result of Bcl-2′s negative effect on cell cycle progression.[5,6] It is this seemingly paradoxical effect of Bcl-2 that we chose to examine.

There are multiple ways in which apoptosis and cell cycle regulation pathways cross.[6] Bcl-2 slows cell proliferation by lengthening the cell cycle.[7,8] Expression of Bcl-2 increases the amount of time cells spend in G_1, thereby slowing the G_1-S transition.[9-12] The exact mechanism of this effect is unknown, however, some cell lines displayed a downregulation of cell cycle inhibitor $p21^{WAF1/CIP1}$,[13] upregulation of inhibitor $p27^{KIP1}$,[12,14] hypophosphorylated retinoblastoma protein (pRb)[15] and reduced active levels of transcription factor E2F.[14]

We are interested in determining what gene expression changes occur upon *Bcl-2* overexpression in MCF10A cells. In this paper, we focus on gene expression changes in cell cycle and cell proliferation genes. Our long-term goal is to shed light on gene expression patterns leading to breast cancer development. Previous studies have demonstrated that *Bcl-2* expression in MCF10A cells causes an altered cell cycle,[10] but this is the first time microarray analysis has been reported.

Since MCF10A cells were immortalized spontaneously from mortal diploid cells, the cell line exhibits characteristics of normal breast epithelium: (a) three-dimensional growth in collagen; (b) control of growth in culture by hormones and growth factors; (c) lack of anchorage-independent growth; (d) dome formation in confluent cultures; and (e) lack of tumorigenicity in nude mice.[16] Several studies have used the MCF10A cell line as a control in breast cancer cell studies, and therefore we hypothesized that MCF10A could substitute for non-transformed cells in culture.[17,18] In fact, the cell line has been the focus of a study to examine cytogenetic changes that occur upon breast cancer progression.[19]

We prepared a stable *Bcl-2*-expressing MCF10A cell line (MCF10A/Bcl-2) by retroviral infection, and showed that MCF10A/Bcl-2 cells had a significantly lower growth rate compared to control MCF10A/Neo cells caused by a slowing of the G_1-S transition of the cell cycle. Subsequently, a cDNA microarray analysis comparing the two cell lines was performed and the data subjected to two separate pathway analysis tools. We hypothesized that *BCL2* overexpression would downregulate genes involved in the G_1-S phase transition, and genes that block cell cycle progression would be upregulated. PAGE identified 22 significantly changed gene sets, and the highest ranked network identified by IPA contained 24 significant genes. By qRT-PCR we confirmed the upregulation of two cell cycle genes, *CCND1* and *CDC42* and the downregulation of the cell cycle phosphatase gene *CDC25A*. However, western analysis did not confirm the upregulation of cyclin D1 protein. In addition, genes for several transcriptional activators of *CCND1* such as *FN1* and *TGFβ3* were also shown to be differentially regulated. Therefore, we demonstrate that *BCL2* overexpression causes phenotypic changes that can be correlated to specific gene expression changes with microarray and pathway analysis, but protein analysis is necessary to confirm their involvement.

NIH-PA Author Manuscript

NIH-PA Author Manuscript

NIH-PA Author Manuscript

Results

Bcl-2 expression and the cell cycle

To verify the successful introduction of our *BCL2* construct, western blot analysis with antibodies to Bcl-2 was performed to determine expression level of the introduced Bcl-2 protein in the MCF-10/Bcl-2 cell line. The MCF10A/Bcl-2 cells expressed Bcl-2, while there was no detectable expression in the parent MCF10A and the MCF10A/Neo cells under the same conditions while the expression of β-actin, which was used as a loading control, was equivalent in all three cell lines (Fig. 1). However, a longer exposure with a higher antibody concentration did result in a positive Bcl-2 signal in MCF10A and MCF10A/Neo cells (data not shown). These results confirm that the *BCL2* construct was successfully introduced and expressed at a high level in the MCF10A/Bcl-2 cell line.

Cell counts were performed by trypan blue exclusion to determine the growth rate for each of our cell lines (Fig. 2). MCF10A (circle) and MCF10A/Neo cells (square) showed similar growth rates with a doubling time of approximately 50 h. MCF10A/Bcl-2 cells (triangle) were observed to have a significantly slower growth rate with a doubling time of approximately 90 h.

We endeavored to determine which stage of the cell cycle was altered in the MCF10A/Bcl-2 cells. We synchronized cells by two different methods. First, cells were grown without growth factors (GF) for five days, and then GF were added. Growth factor addition after synchronization causes cells to enter S phase. Flow cytometry with PI was used to determine the percentage of cells at each phase of the cell cycle. Figure 3A is a graph of the number of MCF10A/Neo cells in each phase as determined by ModFit analysis of flow cytometry data, starting on the day GF were added. Each bar represents counts from an average of three independent experiments carried out in duplicate. Approximately 80% of MCF10A/Neo cells were in G_1 at time 0, after five days GF withdrawal. By 21 h 60% of the cells had left G_1 and were in S or G_2 phase.

Figure 3B is a graph of the same cell cycle analysis done with MCF10A/Bcl-2 cells after GF re-addition. Many cells were floating in the medium during the five days of GF withdrawal but only live (adherent) cells were used for analysis. Ninety percent of MCF10A/Bcl-2 cells were in G_1 five days after GF withdrawal (time zero). In contrast to the MCF10A/Neo cells, the MCF10A/Bcl-2 cells remained in G_1 longer, up to 24 h after GF re-addition. T-tests confirmed that from 18–24 h, the MCF10A/Bcl-2 cell line had a significantly higher number of cells in G_1 vs the MCF10A/Neo cell line. The cells progressed from S phase to G_2 phase during the 24 to 36 h period. However, there seemed to be fewer cells in S and G_2 phases in the MCF10A/Bcl-2 cell line overall compared to the control. Bcl-2 has been implicated in cell cycle exit to G_0, as well as inducing a slow G_1-S transition.[20] Therefore, it appears that the MCF10A/Bcl-2 cells were slow to leave G_1 and enter S and G_2 phase compared to the control cell line, and some cells may have exited into G_0 instead of continuing to cycle.

Cells were also synchronized with the microtubule inhibitor colchicine. Colchicine inhibits microtubule proliferation and arrests cells in the G_2 phase.[21] Cells were treated with 0.1 μM colchicine and stained with PI. The control was untreated cells that were harvested at 70% confluency. Figure 3C is a graph of the cell cycle distribution of MCF10A/Neo cells treated with colchicine. Each bar represents cell counts from three independent experiments carried out in duplicate. Control cells (time 0) were 80% in G_1 at time 0. Colchicine-treated cells began to leave G_1 on day one of treatment. Approximately 60% of MCF10A/Neo cells were in G_2 on day two of treatment and 80% of the cells were in G_2 by day four. On day five the MCF10A/Neo cells started to die, indicated by the sub-G_1 peak (referred to as dead on graph), and there was an increase in death on day four and day five.

NIH-PA Author Manuscript

NIH-PA Author Manuscript

NIH-PA Author Manuscript

Figure 3D is a graph representing the cell cycle distribution of MCF10A/Bcl-2 cells when treated with colchicine. The control was untreated MCF10A/Bcl-2 cells that were harvested at 70% confluency. Control cells (time 0) were 70% in G_1 at time 0. On day two of treatment, t-tests confirmed that there were significantly more cells in G_1 and significantly fewer cells in S and G_2 compared to the same time point in MCF10A/Neo cells (Fig. 3C). Therefore, as with GF withdrawal synchronization, the MCF10A/Bcl-2 cells were slower to leave G_1 than the MCF10A/Neo cells. MCF10A/Bcl-2 cells started dying (as indicated by the sub-G_1 peak) on day three, and there were significantly more dead cells at days three, four and five compared to the same time points of MCF10A/Neo cells. Day four shows 60% of the total events collected (10,000) were sub-G_1, indicating that the cells were dead. Day five had 40% of total events as sub-G_1. This number was lower than day four's total because there was more cellular debris that was not counted as sub-G_1 in the latter. Subsequent analysis showed that this death was apoptotic (data not shown).

Microarray analysis

In order to identify differentially expressed genes, the gene expression profiles of the two cell lines, MCF10A/Neo and MCF10A/Bcl-2, were compared. The raw intensity values from the Phosphoroimager 860 were normalized to allow comparison of values from different arrays using a Z score normalization method.[22] This method ultimately produced a distribution of Z scores for all the genes in each array, and used the differences in the Z scores to calculate Z ratios to locate genes that were expressed differentially.[22,23] Genes that had a Z ratio >1.5 and a p-value <0.05 were considered significant. This narrowed the number of significant genes to 363, including 307 upregulated and 56 downregulated. The data was then analyzed using two functional analysis tools.

Parametric analysis of gene set enrichment (PAGE) uses the fold change between the control and experimental groups to calculate Z scores of predefined gene sets and normal distribution to assign statistical significance to the gene sets.[24] The list of all of the genes used in the array and their Z scores are put into the analysis and Z scores are assigned to the functional groups within each cell line. A list of genes involved in each pathway and their individual Z scores are also displayed in the analysis. Traditional microarray data analysis requires that individual genes have significantly different expression levels in order for them to be considered differentially regulated. PAGE takes into account that genes are co-regulated. Therefore, it is possible that genes individually may not be significant, but significant differences can be demonstrated by grouping genes into gene sets. By looking at groups of genes involved in a specific function, significant differences represent a biologically meaningful result.

The PAGE graph shows Z scores of every significantly changed pathway between the MCF10A/Bcl-2 and MCF10A/Neo cell lines (Fig. 4A). The Z scores for each of these pathways were significantly different because, in most cases, the Z score for the pathway in the other cell line was zero. These pathways included insulin signaling, gross chromosomal rearrangements, DNA repair, and others involved in apoptosis and blocking cell cycle progression.[25] When we looked at the pathways for processes such as glycolysis or gluconeogenesis, common pathways in every cell, we saw no significant difference in the Z scores. In addition, we observed that despite the fact the MCF10A/Bcl-2 cells spent more time in G_1 than the MCF10A/Neo cells, there was no significant difference in the Z score for cell cycle arrest pathway.

Ingenuity Pathway Analysis (IPA) assigns biological functions to genes using the Ingenuity Pathways Knowledge Base (Ingenuity Systems, Inc., Redwood City, CA). The knowledge base comprises over 200,000 full text articles and information about thousands of human, mouse, and rat genes.[26] This information is used to form networks to create an 'interactome' of genes all involved in specific biological processes. IPA groups significant genes according to the

NIH-PA Author Manuscript

NIH-PA Author Manuscript

NIH-PA Author Manuscript

biological processes in which they function. The program displays the genes' significance values, the other genes with which it interacts, and how the genes' products directly or indirectly act on each other, including those not involved in the microarray analysis.[26,27] The networks created are ranked depending on the number of significantly expressed genes they contain. The highest ranked network identified by IPA contained 24 significant genes (Fig. 5). This network includes genes whose products function in controlling the cell cycle, cell proliferation, metastasis, and angiogenesis.

From this network, eight genes, *AGT*, *AKR1C3*, *CDC25A*, *CYR6*, *FN1*, *MMP1*, *TGF*β*3* and *TGF*β*I*, were selected for further analysis, in addition to *CDC42* and *CCND1* (Fig. 5B) (Table 1). We chose genes that were limited to those significantly expressed genes and their transcription factors that are necessary for cell proliferation and cell cycle progression. These genes were then located in the PAGE analysis to determine how the two analysis tools compared (Fig. 4B). Three of the target genes identified in the network analysis by IPA were not found in the PAGE analysis results: *AKR1C3*, *TGF*β*I* and *MMP1*. However, the other six genes and *BAX* were found in ten different pathways. *CDC42*, *CDC25A* and *CCND1* were all found in the glutamate downregulation pathway (Glut Down), while only *CDC42* and *CDC25A* were found in the rapamycin downregulation pathway (Rap Down). *CDC25A* was also found in the pathway that involves the activation of Src by protein-tyrosine phosphatase alpha (srcRPTP Pathway). All of the other target genes showed no pathways in common. TGFβ3 alone was found in the estrogen receptor modulators downregulated signature gene set (Frasor ER Down). *CYR61* was in the GNF female genes set, while *FN1* was found in the G13 signaling pathway and the hematopoesis related transcription factor gene set (Hemo-TF-List-JP). *BAX* was found in a total of three gene sets, including the Bcl-2 family and regulatory network, the mitochondria apoptotic pathway, and the radiation sensitivity gene set. *AGT* was not pursued as it could not be confirmed by qRT-PCR (see below).

qRT-PCR analysis

Quantitative reverse transcription PCR (qRT-PCR) was performed with primers specific for each target gene to verify changes in gene expression between the MCF10/Neo and the MCF10/Bcl-2 cell lines. The fold-change values for each target gene are shown in Table 1. Genes that were overexpressed according the microarray showed a 3–11 fold increase in expression in the MCF10A/Bcl-2 cell line by qRT-PCR (Fig. 6). In addition, *Bcl-2* was overexpressed approximately 800-fold (data not shown). Genes that were under-expressed showed a 0.29–0.59 fold decrease in expression in the MCF10A/Bcl-2 cell line (Fig. 6). One gene, *AGT*, from the network shown in Figure 5B could not be amplified by qRT-PCR even though two sets of primers were attempted.

Western analysis

We carried out western analysis of several proteins with commercially-available antibodies (Fig. 7). Several antibodies did not show any bands (data not shown). We attribute this result to a low expression level of these proteins, or lack of specificity of the antibody. Bax, Cdc42, and Fn1 were slightly overexpressed in MCF10A/Bcl-2 cells. Cyclin D1 did not show overexpression in MCF10A/Bcl-2 cells, although the mRNA was overexpressed 8-fold by qRT-PCR (Table 1).

Discussion

In general, studies that have examined Bcl-2′s cell cycle effects have hypothesized that Bcl-2 affects the kinetics of cell cycle progression at the G_1-S transition.[9-12] Specifically, Lin et al., showed that Bcl-2 slows the cell cycle and increases cyclin D1 expression, and used reporter plasmids to show that Bcl-2 induces cyclin D1 promoter activity.[10] Our study has followed

NIH-PA Author Manuscript

NIH-PA Author Manuscript

NIH-PA Author Manuscript

up on these findings with microarray analysis to arrive at a possible gene expression pattern that accounts for the phenotypic changes that occur upon Bcl-2 overexpression. Like their cell line, ours exhibited significantly slower proliferation compared to the control MCF10A/Neo cells, and we showed they were slowed in the transition between the G_1 and S phases.

A cDNA microarray comparing the MCF10A/Neo and the MCF10A/Bcl-2 cell lines produced 363 significantly changed genes. In order to determine which genes were of interest in the understanding of the altered cell cycle phenotype, we analyzed the Z score and Z ratio data with two pathway analysis tools. PAGE showed that several pathways were up or downregulated equally in both cell lines. This result could be due to the growth conditions for the cells, since they are grown in the presence of factors such as epidermal growth factor, insulin and cholera toxin. There were 22 gene sets that were differentially regulated between the two cell lines. Clearly these results indicate that there are multiple pathways that are affected by the overexpression of this one gene. IPA also produced multiple networks of interacting genes, many of which were differentially expressed between the two cell lines. We selected differentially expressed genes that were found in the most highly rated IPA network, as well as some of the other networks and are directly involved in controlling the cell cycle and proliferation for further analysis. When we determined which PAGE pathways or gene sets contained target genes, some appeared in the same pathways, others were found alone. However, only two of the genes, *TGF*β*3* and *FN1*, were found in two pathways that were differentially expressed, and the rest of the genes were found in pathways that were not significantly different between the cell lines. Therefore, in our analysis, there does not seem to be a relationship between the gene sets identified by PAGE and the network from IPA. This result may be due to the different methods for choosing genes that belong to any given pathway.

The mRNA expression levels of all of the genes that we analyzed positively correlated with the microarray data. In addition, we carried out qRT-PCR on *BCL2* and *BAX*, and those results also correlated with the microarray data. Our results give us confidence that the microarray data is accurately reflecting transcriptional differences between the MCF10A/Neo and MCF10A/Bcl-2 cell lines. However, the western blot results did not show that protein expression correlated with mRNA expression in all cases. In addition, we were not able to detect several proteins by western blot, although we used higher concentration of the antibody than suggested. Tools for mRNA analysis are more robust than tools for protein analysis; western blotting is a technique that relies on antibodies that are highly variable, and therefore it is difficult to use as a quantitative method. However, in the following discussion we will attempt to integrate our results to arrive at a gene and protein expression pattern that may explain the slow-growth phenotype observed.

CDC25A

Cdc25A is a phosphatase that promotes cell cycle progression by activating G_1 cyclin dependent kinases and has been postulated to be an oncogene.[28] Recently, Cdc25A has been proposed to control the balance between proliferation and checkpoint response in the presence of specific neu/ras oncogene activation.[29] The Cdc25A phosphatase removes inhibitory phosphates from tyrosine and threonine residues of Cdk2.[28,30] This dephosphorylation is necessary for S phase initiation.[31] In a study that sampled breast carcinomas, high levels of *CDC25A* mRNA were seen in 47% and were associated with poor prognosis.[30] The same study showed that *CDC25A* allows MCF7, a breast cancer epithelial cell line, to progress into the S phase. In these cells that overexpress *CDC25A* there is also a higher level of Cdk2 enzymatic activity. It was also shown that when MCF7 cells are transfected with antisense oligonucleotides for *CDC25A* to decrease *CDC25A* expression, there is a subsequent decrease in Cdk2 activity. This data suggests that Cdc25A is required to maintain Cdk2 activity in MCF7 cells.

NIH-PA Author Manuscript

NIH-PA Author Manuscript

NIH-PA Author Manuscript

The microarray analysis shows that in the MCF10A/Bcl-2 cell line, *CDC25A* is significantly downregulated, to 30% of that present in the control (Table 1, Fig. 6). This low level of expression may be insufficient to carry out complete dephosphorylation of Cdk2 to allow progression to S phase. Therefore, it is possible that the low levels of *CDC25A* mRNA are the primary reason for the slow growth phenotype observed in MCF10A overexpressing Bcl-2.

As to mechanism of transcriptional regulation of *CDC25A*, cell cycle progression occurs upon phosphorylation of pRb, which binds to E2F when dephosphorylated and prevents E2F from functioning as a transcription factor. E2F-regulated genes include *CDC25A*.[32] However, complete phosphorylation of pRb and activation of E2F requires both cyclin D-Cdk4/6 and cyclin E-Cdk2 activities.[33] Bcl-2 has been shown to directly bind Cdk2, reducing its kinase activity which leads to hypophosphorylated pRb and inhibition of E2F.[34] Therefore, downregulation of *CDC25A* in MCF10A/Bcl-2 cells may be attributed to inhibition of E2F.

CDC42

As Cdc42 is slightly overexpressed at the protein level, it may have a role in the slow-growth phenotype. Cdc42 is a member of the Rho family of small GTPases that have roles in organizing the actin cytoskeleton and cell cycle progression.[35] Cdc42 involvement in the cell cycle includes spindle assembly and positioning, micro-tubule-kinetochore attachment, promoting the G_1/S progression in a variety of cell types, and activating a signal transduction pathway that controls the polarity of the microtubules during mitosis.[35-38] It has been hypothesized that Cdc42 is sufficient to cause anchorage-independent cell cycle progression in mouse embryonic fibroblasts.[39] Cdc42 functions through modulation of p38 MAPK, and it was found that in non-adherent cells, p38 activity was impaired, thus allowing cell cycle progression.[39] However, Cdc42 has also been shown to inhibit cell proliferation in NIH 3T3 cells by causing arrest in G_1.[40] In these cells, the expression of *CDC42* increased the levels of activated p38. p38 can cause cells to undergo cell cycle arrest, as it activates a stress pathway that inhibits cell cycle progression. It was proposed that Cdc42 and p38 could prevent the cell from progressing into the S phase by inhibiting G_1 cyclins. We conclude that one effect of the overexpression of *BCL2* in MCF10A cells is a subsequent slight increase in Cdc42 levels that raise active p38 levels and contribute to a slowed cell cycle progression. Such overexpression of Cdc42 may also lead to chromosomal instability.

Cyclin D1, Fn1 and TGFβ3

CCND1 is an oncogene that is commonly overexpressed in tumors,[41] however, its expression is not associated with increased tumor proliferation.[42] However, cyclin D1 has been shown to play a role in cell migration that is required for tumor metastasis through inhibition of expression of the ECM protein TSP-1.[29,38,43] Lin et al., suggested that Bcl-2 induces *CCND1* expression by causing the activation of the promoter, through activation of focal adhesion kinase (FAK).[10] They showed that *BCL2* overexpression in MCF10A cells caused FAK to be more efficiently activated regardless of cell anchorage. These results suggest that *BCL2* caused the upregulation of *CCND1* through a cell adhesion-signaling pathway.[10]

There a number of mechanisms as to how FAK could promote *CCND1* transcription. In NIH3T3 fibroblasts, FAK increases the transcription of *CCND1* by enhancing the binding of an Ets transcription factor to the Ets B element of the *CCND1* promoter.[44] *CCND1* transcription is also induced by an interaction between fibronectin (Fn1) and FAK.[18] That interaction transmits a signal to Rac, inducing *CCND1* transcription. Fn1 is present in the ECM, plasma membrane, and cytoplasm and is specifically involved in stromal matrices, which are commonly found at the site of injury and inflammation.[18] Components of the ECM have a widespread effect on proliferation and differentiation of cells in culture, and the ability of the cells to grow independently of cell matrix interactions is a major event in malignant

NIH-PA Author Manuscript

NIH-PA Author Manuscript

NIH-PA Author Manuscript

transformations.[45] Although *FAK* was not significantly increased, the microarray data and qRT-PCR did show an increase in *FN1* expression in the MCF10A/Bcl-2 cell line, and slight overexpression at the protein level. There was also a significant increase in the levels of *TGFβ3*, which stimulates the transcription of *FN1*,[18,46] although we were unable to detect Tgfβ3 by western blot. Therefore, the increase in *CCND1* expression could be through FAK-Fn1 signaling through Rac.

Our results differ from Lin et al.[10] in that we did not see overexpression of cyclin D1 at the protein level. It may be that our lysate preparation for the western blot was not exactly the same, and that under some conditions we also may see overexpression of cyclin D1. Nevertheless, we both showed a slow cell cycle upon *BCL2* overexpression in MCF10A cells. Since other proteins change in levels of expression that could be responsible for the phenotype, and since it has been reported that overexpression of *CCND1* is does not always affect cell proliferation in vivo,[42] and in vitro,[47,48] we attribute our slow cell cycle phenotype to changes in expression of other proteins besides cyclin D1.

Our western analysis shows that Fn1 and Cdc42 are only slightly overexpressed, and cyclin D1 is not overexpressed at the protein level. There may be a feedback mechanism at the translational or post-translational level that results in maintaining levels of these proteins in spite of overexpression of the mRNA. In fact, proapoptotic Bax is probably similarly regulated, albeit in the opposite direction, as *BAX* is slightly downregulated at the mRNA level (Fig. 6), but there is increased Bax protein (Fig. 7). Others have reported that overexpression of *BCL2* causes a consequential increase in Bax levels by stabilizing the Bax protein.[49] Cyclin D1 has been shown to be post-translationally regulated by both ubiquitin-dependent and -independent degradation pathways.[50] Therefore, it is possible that in our cell line, these pathways are altered upon *BCL2* overexpression to function in maintaining cyclin D1 at steady-state levels. The same type of mechanism may be at work for other proteins such as Cdc42 also, as mRNA abundance is almost 5-fold higher in the MCF10A/Bcl-2 cell line, but protein is only slightly overexpressed. Our inability to see large differentials in protein expression also may be because western analysis, since it relies on detection of binding events by two antibodies, is not as quantitative as techniques such as qRT-PCR. Finally, as most of our proteins are involved in the cell cycle, it may be that steady state levels are only slightly changed, but the kinetics of expression are altered, which we would only detect by western analysis of lysates taken from a time-course of synchronized cells.

Besides an inhibition of E2F-mediated gene transcription, there are several possible mechanisms whereby Bcl-2 affects transcription. Bcl-2 has been shown to regulate NFAT-transcription factor in T cells and this effect is Ca^{2+}-mediated.[51] Bcl-2 is known to affect Ca^{2+} homeostasis in the ER and mitochondria.[52,53] Ca^{2+} is a known modulator of transcription, as it has been shown to regulate c-Src through binding to calreticulin which affects *FN1* transcription.[54] In addition, Bcl-2 blocks p53-dependent apoptosis, specifically the transcriptional repression function of p53, while leaving the transcriptional activation function of p53 intact.[55,56] This effect may be due to binding by Bcl-2 to the transcriptional repressor Btf.[57] Similarly, Bcl-2 modifies the transcriptional repressor function of the glucocorticoid receptor, which directly binds the transcriptional activator AP-1 to block its effects.[58] Therefore, Bcl-2 allows the glucocorticoid receptor to remain active as a transcriptional activator. Bcl-2 has been shown to downregulate the transcriptional activity of NFκB, a transcription factor involved in cell death.[59] A proapoptotic Bcl-2 family member, Bad, has been shown to interact with c-Jun to inhibit transcription of cyclin D1 in breast cancer cells.[60] Finally, a viral Bcl-2 homolog, adenovirus E1B 19-kDa protein, has demonstrated similar transcriptional activities.[56] In addition, E1B has been shown to act as an enhancer-dependent transcriptional activator for various promoters,[61] and specifically activates c-Jun

NIH-PA Author Manuscript

NIH-PA Author Manuscript

NIH-PA Author Manuscript

mediated transcription.[62] A similar role for Bcl-2 could potentially cause large numbers of genes to be upregulated, as we see occurring in our MCF10A/Bcl-2 cell line.

In summary, the overexpression of *BCL2* in MCF10A cells showed a large effects on a number of genes that are involved in the cell cycle. We expected *BCL2* to downregulate genes that were involved in cell cycle progression and this was observed with *CDC25A*. However, this effect was not observed with *CCND1*, which normally is associated with increased cell cycle progression, but the level of cyclin D1 protein was maintained. Although *CDC42* can stimulate the cell cycle, its overexpression is also associated with G_1 arrest, which supports the slow-growth phenotype observed. Finally, the reduction of *CDC25A* expression alone may be sufficient to slow the cell cycle. Our results give a slight cautionary note to interpretation of microarray and qRT-PCR results, as several genes that were found to be overexpressed by these methods show compensatory changes that result in reduced levels of protein. In addition, several of our antibodies did not detect any protein, although the mRNA is present in the cell. Western analysis may not be sensitive enough for some proteins to detect changes at the mRNA level. In a similar study of overexpression of oncogenes in breast epithelial cells, some protein markers were not readily detected by western analysis.[63]

Materials and Methods

Cell culture

MCF10A cells were obtained from the Karmanos Cancer Institute (Detroit, MI). For routine culturing, the cells were maintained as subconfluent monolayers at 37°C and 5% CO_2 in Dulbecco's modified Eagle's medium/Ham's F-12 nutrient mixture (DMEM/F-12), containing 15 mM HEPES and 2.5 mM L-glutamine, supplemented with 5% heat inactivated equine serum, 500 ng/ml hydrocortisone, 21.5 ng/ml epidermal growth factor (EGF), 10 μg/ml insulin, 100 ng/ml cholera toxin, and 10 μg/ml gentamicin (hereafter referred to as DMEM/F-12 complete). MCF10A/Bcl-2 and MCF10A/Neo were grown under the same conditions.

Reagents

DMEM/F-12, L-glutamine, and HEPES were obtained from MediaTech. Epidermal growth factor, hydrocortisone, insulin, and staurosporine were acquired from Sigma. Equine serum was obtained from Bio-Witaker. Gentamicin was obtained from Invitrogen. All other reagents were from Fisher Scientific unless otherwise noted.

Construction of cell lines

An MCF10A cell line that stably overexpresses *BCL2* and an MCF10A vector control cell line were produced by infection of MCF10A cells with a retroviral vector containing either murine *BCL2* under control of the SV40 promoter and neomycin resistance (*neo*^{r}) genes (PA317/Bcl-2) or *neo*^{r} (pZip/Neo) alone as described.[66] Briefly, MCF10A cells were infected with 1×10^6 PA317/Bcl-2 virus particles or 1×10^5 pZip/Neo virus particles in the presence of 10 μg/ml of polybrene (Sigma) for 4 h. Cells stably expressing *BCL2* and the neomycin resistance marker (MCF10A/Bcl-2) or the neomycin resistance marker alone (MCF10A/Neo) were selected by growth in DMEM/F-12 medium supplemented with 2 mg/ml of the neomycin analog G418 (Invitrogen). Several neomycin resistant clones from each infection were pooled, thus minimizing artifacts from gene insertion into a specific site.

Proliferation assay

Cells were seeded at a concentration of 100,000 cells per 35 mm dish in complete medium. Cell counts were determined every 24 h for 10 days. Viable cells were counted by trypan blue exclusion as follows. Cells were harvested by trypsinization in 0.1% trypsin/1.06 mM EDTA

NIH-PA Author Manuscript

NIH-PA Author Manuscript

NIH-PA Author Manuscript

in Hanks Balanced Salt Solution (Invitrogen) and collected by centrifugation. The cells were resuspended in 1 ml PBS. 200 μl of cell suspension was added to 600 μl of PBS and 200 μl of a 0.4% trypan blue stain (GIBCO). Ten μl of cell suspension was added to each side of a Bright-line hemocytometer. The cells were counted under 400x magnification. The results were graphed with Microsoft Excel, and unpaired t-tests were used to determine significant differences ($p < 0.025$).

Cell synchronization and flow cytometry

Synchronization via growth factor withdrawal—Subconfluent monolayers in 75 cm^2 flasks were washed twice with 10 ml of PBS containing 1 mM EDTA. Pre-warmed growth factor (GF) withdrawal media (DMEM/F-12 with 15 mM HEPES, 2.5 mM L-glutamine and 10 μg/ml gentamicin) (10 ml) was then added to each flask. After 5 days of GF withdrawal, media was removed and complete media was added. Cells were harvested by trypsinization at 0, 12, 15, 18, 21, 24, 30 and 36 h after complete media addition. Cells were then prepared for flow cytometric analysis.

Synchronization via colchicine—Cells were washed twice with 10 ml of PBS, then 10 ml of complete media with 0.1 μM colchicine (Sigma) was placed on the cells (time 0), and cells were harvested by trypsinization at 1, 2, 3, 4 and 5 days. Cells were then prepared for flow cytometric analysis.

At each time point, the cells were centrifuged at 200 × g for 5 min and the supernatant was removed. The cells were washed once with PBS, and resuspended in 1 ml of complete media. The cells were fixed by passage through a 23 g needle into cold 70% ethanol. The cells were stored at −20°C until all samples were collected. The cells were centrifuged and then washed in 1 ml PBS. RNase (10 μl of 1 mg/ml) was added and incubated at 37°C for 30 min then washed with PBS. Cells were then resuspended in 1 ml PBS and 10 μl of a 1 mg/ml propidium iodide (PI), incubated in the dark for 30 min at RT, then placed on ice and analyzed on a FACScan flow cytometer (Beckton Dickinson). Ten thousand events were captured and the analysis was performed on Modfit v. 3.1. Unpaired t-tests were carried out to determine significant differences between the two cell lines at each time point ($p < 0.05$).

Microarray analysis

RNA was prepared using the Totally RNA™ Kit (Ambion). Samples were treated for possible DNA contamination with the Turbo DNA-free kit from Ambion. The purity and quantity of the RNA was determined by measuring the A_{260}/A_{280} ratio on a BioPhotometer (Eppendorf). The human cDNA array consisted of full-length cDNA clones generated by the National Cancer Institute's Mammalian Gene Collection. The cDNA arrays developed from these clones consist of 9600 features, with 1152 blank spots. Each membrane contained 384 sub arrays with 24 genes on each sub array. Each spot represented an individual gene, thus the array incorporated over 9000 unique genes. Total RNA was radioactively labeled with [α ^{33}P] dCTP. Details of the labeling and array protocols have been described.[67] Briefly, total RNA (20 μg) was reverse-transcribed to cDNA with reverse-transcriptase enzyme in the presence of [α ^{33}P] dCTP. The [α ^{33}P] dCTP-cDNA was purified through a spin column by size separation (BioSpin, Bio-Rad) from [α ^{33}P] dCTP and the heat denatured probe (5×10^6 cpm) was diluted in 4 ml of Microhyb solution (RG) and hybridized to the array for 16–18 h at 50°C with rotation. The target cDNA was spotted on the nylon membranes and hybridized overnight at 50°C with labeled probe cDNA from each cell line. cDNA from each cell line was arrayed in triplicate. Hybridized arrays were rinsed in 2 X SSC and 0.1% SDS twice at 55°C. The microarrays were exposed to phosphor screens for 1–3 days, and then scanned with the Phosphorimager 860 at 50 μm pixel resolution. ArrayPro software was used to convert the hybridization signals into

NIH-PA Author Manuscript

NIH-PA Author Manuscript

NIH-PA Author Manuscript

raw intensity values, which was then transferred to a Microsoft Excel spreadsheet for further analysis.

Array data analysis and analysis tools

In order to compare the array data between the two cell lines, the raw intensities values were normalized using Z transformation.[22] The following equation was used to calculate Z scores of each raw value:

$$Z\ \text{score}_{(G_1)} = \left[\ln\left(\text{raw intensity}_{G_1}\right) - \ln\left(\text{mean raw intensity}_{G_1 \ldots G_n}\right)\right] / \left[\text{std dev}\left(\ln\left(\text{raw intensity}_{G_1 \ldots G_n}\right)\right)\right]$$

where G_1 represents any gene on the microarray and $G_1 \ldots G_n$ represents the measure of all the genes on the microarray. The natural logarithm was used to decrease the variance and put the data on small scale. Genes whose average intensity between the two treatments was greater than zero were eliminated from further calculations. In addition, genes of low intensity compared to background, showing a high fold change, were also eliminated.[23] Gene expression differences between the two arrays were calculated using the following equations:

$$Z\ \text{difference}_{(G_1)} = Z\ \text{score}_{(G_1,\text{Neo})} - Z\text{score}_{(G_1,\text{Bcl-2})}$$
$$Z\ \text{ratio} = Z\ \text{difference}_{(G_1)} / \text{Std dev}_{(Z\ \text{difference}\ G_1 \ldots G_n)}$$

where G_1, Neo represents the Z score for a gene in the MCF10A/Neo cell line and G_1, Bcl-2 represents the Z score for the same gene in the MCF10A/Bcl-2 cell line. The Z ratios were used as a measure of fold-change between the two cell lines. p values were calculated from the filtered genes, using t-tests, to test for repeatability among the replicate arrays. Only the genes having a p-value <0.05 are and having a Z ratio >1.5 were used in further analysis. The standard deviation of the Z difference of all the genes on the array was used to determine whether a given ratio was statistically significant considering the array as a whole. Parametric analysis of gene set enrichment (PAGE) a module of DIANE software, a microarray analysis platform, was used to identify groups of genes that were significantly enhanced.[24,25] Ingenuity Pathway Analysis (IPA) was used to determine the biological pathways in which the genes that were over or under expressed significantly were involved.[26]

Quantitative reverse transcription PCR

Vector NTI (Invitrogen) was used to display the mRNA sequence of target genes (Table 2). A 300 bp sequence that crosses an intron-extron junction was selected and subjected to BLAST analysis to ensure there was no homology with other genes.[68] The sequence was pasted into Mfold to determine how the mRNA would fold at the specific annealing temperature.[69,70] The annealing temperature that was used for all of the primers was 55°C. Primer3 was used to select the appropriate forward and reverse primers that would avoid the secondary structure of the RNA and minimize the formation oligo-duplexes.[71] The primers were all 19–23 bp in length and produced amplicons of 72–150 bp (Table 2).

cDNA for qRT-PCR was prepared with the RETROscript kit from Ambion. Reverse transcription was performed using 1 μg of total RNA. To confirm the microarray results, quantitative RT-PCR (qRT-PCR) was performed from cDNA. GAPDH served as the control in each qRT-PCR reaction. The reactions were carried out on an Icycler IQ (BioRad). Each 25 μl PCR reaction included SYBR Green Supermix (Bio Rad), containing 0.4 mM each of dATP, dCTP, dGTP and dTTP, 50 U/ml iTaq DNA polymerase, 6 mM Mg^{2+}, SYBR Green I, 20 nM fluoroscein, and stabilizers. The reaction also contained cDNA from one cell line and the

NIH-PA Author Manuscript

NIH-PA Author Manuscript

NIH-PA Author Manuscript

forward and reverse primers specific for the gene of interest. The efficiency of each primer set was calculated using a standard curve. Dilutions of cDNA ranging from 0.37–30 ng were prepared and the cycle threshold (C_t) values for the reactions were plotted against the cDNA concentrations. The slope of the line was used in the following equation: $E = 10^{(-1/slope)}$ to calculate the efficiencies. All efficiencies were greater than 90%. We used the comparative cycle threshold method ($2^{-\Delta\Delta C_t}$) to quantify gene expression.[72] Each PCR reaction was carried out on at least two separate cDNA preparations. Fold-change values represent an average of the two separate experiments. Each reaction was normalized to the housekeeping gene (GAPDH) with the following equation:

$$\text{Fold change} = 2^{\hat{}-(C_t bcl-2 - C_t\ GAPDH)-(C_t neo - C_t\ GAPDH)}$$

Western blotting

Cells were lysed by vortexing on ice in 50 mM Tris (pH 7.4), 150 mM NaCl, 1 mM EDTA, 1% Triton X-100, 1 mM PMSF, 1% protease inhibitor cocktail (Sigma). Protein concentrations were determined by the Bradford method (BioRad).[73] Discontinuous SDS-PAGE was carried out using the X-Cell SureLock system (Invitrogen). Total cellular protein (50 μg) was separated on SDS-polyacrylamide gels, then transferred to Immobilon-P^{sq} polyvinylidene difluoride (PVDF) membranes (Millipore). For immunodetection the membranes were incubated in blocking buffer (5% non-fat dry milk dissolved in Tris-buffered saline solution with 0.05% Tween-20 (TBS-T)) for 60 min at RT to block all non-specific binding sites. The membranes were then incubated with the primary antibody diluted in blocking buffer for 60 min at RT. After the primary antibody incubation the membranes were washed in TBS-T. The membranes were then incubated with the horseradish peroxidase conjugated secondary antibody for 60 min at RT, then washed in TBS-T. Proteins were visualized by enhanced chemiluminescence plus (ECL^+) system (Amersham) on a FluorChem 8900 imaging system (Alpha Innotech). Antibodies were obtained from Santa Cruz Biotechnology, Inc., (Santa Cruz, CA) or Developmental Studies Hybridoma Bank (University of Iowa, Iowa City).

Conclusion

Multiple pathways are affected by *BCL2* overexpression in breast epithelial cells, and more than one gene is likely responsible for the slow-growth phenotype observed. However, although we saw excellent correlation between the microarray and qRT-PCR results, the protein expression data did not always correlate. This finding may implicate translational and post-translational regulation mechanisms in maintaining steady-state protein levels.

It appears that *BCL2* has evolved the ability to block apoptosis along with slowing the cell cycle, thus working in conjunction with other oncogenes to promote tumorigenesis.[6,64] *BCL2*'s multiple functions in its role as a proto-oncogene is not surprising, given the fact that many proteins that have one function may be co-opted for other functions that promote cancer.[64,65] As a mitochondrial protein, it has been suggested that Bcl-2 may act in conflict with the nuclear genome (intragenomically) in promoting cancer at the expense of the organism.[65]

Acknowledgements

The authors would like to thank Megan Hadden for help with the microarray hybridization and Matthew M. Smith for technical assistance. This research was supported in part by the Intramural Research Program of the NIH, National Institute on Aging, and in part by grants from the National Cancer Institute (1R15CA87810-01) to MAF and (R01CA098195) to JAM. The TGFβ3 and Fn1 antibodies developed by Raymond Runyan and Robert J. Klebe, respectively, were obtained from the Developmental Studies Hybdridoma Band developed under the auspices of the NICHD and maintained by The University of Iowa, Department of Biological Sciences, Iowa City, IA 52242.

NIH-PA Author Manuscript

NIH-PA Author Manuscript

NIH-PA Author Manuscript

Abbreviations

Bp, base pair
BLAST, basic local alignment search tool
Bcl-2, B cell lymphoma-2
Ct, cycle threshold
EtBr, ethidium bromide
GF, growth factors
IPA, ingenuity pathway analysis
PI, propidium iodide
PAGE, parametric analysis of gene set enrichment
TBS, tris-buffered saline
qRT-PCR, quantitative reverse-transcription polymerase chain reaction

References

1. Schorr K, Li M, Krajewski S, Reed JC, Furth PA. Bcl-2 gene family and related proteins in mammary gland involution and breast cancer [In Process Citation]. J Mammary Gland Biol Neoplasia 1999;4:153–64. [PubMed: 10426394]
2. Vaux DL, Cory S, Adams JM. Bcl-2 gene promotes haemopoietic cell survival and cooperates with c-myc to immortalize pre-B cells. Nature 1988;335:440–2. [PubMed: 3262202]
3. Ruvolo PP, Deng X, May WS. Phosphorylation of Bcl2 and regulation of apoptosis. Leukemia 2001;15:515–22. [PubMed: 11368354]
4. Abdulkader I, Sanchez L, Cameselle-Teijeiro J, Gude F, Chavez JE, Lopez-Lopez R, et al. Cell cycle-associated markers and clinical outcome in human epithelial cancers: a tissue microarray study. Oncol Rep 2005;14:1527–31. [PubMed: 16273250]
5. Yin XM. Bid, a BH3-only multi-functional molecule, is at the cross road of life and death. Gene 2006;369:7–19. [PubMed: 16446060]
6. Maddika S, Ande SR, Panigrahi S, Paranjothy T, Weglarczyk K, Zuse A, et al. Cell survival, cell death and cell cycle pathways are interconnected: implications for cancer therapy. Drug Resist Updat 2007;10:13–29. [PubMed: 17303468]
7. O'Reilly LA, Huang DC, Strasser A. The cell death inhibitor Bcl-2 and its homologues influence control of cell cycle entry. Embo J 1996;15:6979–90. [PubMed: 9003774]
8. Knowlton K, Mancini M, Creason S, Morales C, Hockenbery D, Anderson BO. Bcl-2 slows in vitro breast cancer growth despite its antiapoptotic effect. J Surg Res 1998;76:22–6. [PubMed: 9695733]
9. Borner C. Diminished cell proliferation associated with the death-protective activity of Bcl-2. J Biol Chem 1996;271:12695–8. [PubMed: 8663032]
10. Lin HM, Lee YJ, Li G, Pestell RG, Kim HR. Bcl-2 induces cyclin D1 promoter activity in human breast epithelial cells independent of cell anchorage. Cell Death Differ 2001;8:44–50. [PubMed: 11313702]
11. Lopez-Diazguerrero NE, Lopez-Araiza H, Conde-Perezprina JC, Bucio L, Cardenas-Aguayo MC, Ventura JL, et al. Bcl-2 protects against oxidative stress while inducing premature senescence. Free Radic Biol Med 2006;40:1161–9. [PubMed: 16545683]
12. Greider C, Chattopadhyay A, Parkhurst C, Yang E. BCL-x(L) and BCL2 delay Myc-induced cell cycle entry through elevation of p27 and inhibition of G_1 cyclin-dependent kinases. Oncogene 2002;21:7765–75. [PubMed: 12420213]
13. Upadhyay S, Li G, Liu H, Chen YQ, Sarkar FH, Kim HR. bcl-2 suppresses expression of $p21^{WAF1/CIP1}$ in breast epithelial cells. Cancer Res 1995;55:4520–4. [PubMed: 7553620]
14. Vairo G, Soos TJ, Upton TM, Zalvide J, DeCaprio JA, Ewen ME, et al. Bcl-2 retards cell cycle entry through p27(Kip1), pRB relative p130, and altered E2F regulation. Mol Cell Biol 2000;20:4745–53. [PubMed: 10848600]
15. Mazel S, Burtrum D, Petrie HT. Regulation of cell division cycle progression by bcl-2 expression: a potential mechanism for inhibition of programmed cell death. J Exp Med 1996;183:2219–26. [PubMed: 8642331]

NIH-PA Author Manuscript NIH-PA Author Manuscript NIH-PA Author Manuscript

16. Soule HD, Maloney TM, Wolman SR, Peterson WD Jr, Brenz R, McGrath CM, et al. Isolation and characterization of a spontaneously immortalized human breast epithelial cell line, MCF-10. Cancer Res 1990;50:6075–86. [PubMed: 1975513]
17. Rodriguez-Mora OG, LaHair MM, McCubrey JA, Franklin RA. Calcium/calmodulin-dependent kinase I and calcium/calmodulin-dependent kinase kinase participate in the control of cell cycle progression in MCF-7 human breast cancer cells. Cancer Res 2005;65:5408–16. [PubMed: 15958590]
18. Wu M, Wu ZF, Kumar-Sinha C, Chinnaiyan A, Merajver SD. RhoC induces differential expression of genes involved in invasion and metastasis in MCF10A breast cells. Breast Cancer Res Treat 2004;84:3–12. [PubMed: 14999149]
19. Worsham MJ, Pals G, Schouten JP, Miller F, Tiwari N, van Spaendonk R, et al. High-resolution mapping of molecular events associated with immortalization, transformation, and progression to breast cancer in the MCF10 model. Breast Cancer Res Treat 2006;96:177–86. [PubMed: 16319984]
20. Vairo G, Innes KM, Adams JM. Bcl-2 has a cell cycle inhibitory function separable from its enhancement of cell survival. Oncogene 1996;13:1511–9. [PubMed: 8875989]
21. Gajate C, Barasoain I, Andreu JM, Mollinedo F. Induction of apoptosis in leukemic cells by the reversible microtubule-disrupting agent 2-methoxy-5-(2′,3′,4′-trimethoxyphenyl)-2,4,6-cycloheptatrien-1-one: protection by Bcl-2 and Bcl-X(L) and cell cycle arrest. Cancer Res 2000;60:2651–9. [PubMed: 10825137]
22. Cheadle C, Fan J, Cho-Chung YS, Werner T, Ray J, Do L, et al. Control of gene expression during T cell activation: alternate regulation of mRNA transcription and mRNA stability. BMC Genomics 2005;6:75. [PubMed: 15907206]
23. Vawter MP, Crook JM, Hyde TM, Kleinman JE, Weinberger DR, Becker KG, et al. Microarray analysis of gene expression in the prefrontal cortex in schizophrenia: a preliminary study. Schizophr Res 2002;58:11–20. [PubMed: 12363385]
24. Kim SY, Volsky DJ. PAGE: parametric analysis of gene set enrichment. BMC Bioinformatics 2005;6:144. [PubMed: 15941488]
25. Subramanian A, Tamayo P, Mootha VK, Mukherjee S, Ebert BL, Gillette MA, et al. Gene set enrichment analysis: a knowledge-based approach for interpreting genome-wide expression profiles. Proc Natl Acad Sci USA 2005;102:15545–50. [PubMed: 16199517]
26. Calvano SE, Xiao W, Richards DR, Felciano RM, Baker HV, Cho RJ, et al. A network-based analysis of systemic inflammation in humans. Nature 2005;437:1032–7. [PubMed: 16136080]
27. Liu J, Xie Y, Ducharme DM, Shen J, Diwan BA, Merrick BA, et al. Global gene expression associated with hepatocarcinogenesis in adult male mice induced by in utero arsenic exposure. Environ Health Perspect 2006;114:404–11. [PubMed: 16507464]
28. Zou X, Tsutsui T, Ray D, Blomquist JF, Ichijo H, Ucker DS, et al. The cell cycle-regulatory CDC25A phosphatase inhibits apoptosis signal-regulating kinase 1. Mol Cell Biol 2001;21:4818–28. [PubMed: 11416155]
29. Ray D, Kiyokawa H. CDC25A levels determine the balance of proliferation and checkpoint response. Cell Cycle 2007;6:3039–42. [PubMed: 18073536]
30. Cangi MG, Cukor B, Soung P, Signoretti S, Moreira G Jr, Ranashinge M, et al. Role of the Cdc25A phosphatase in human breast cancer. J Clin Invest 2000;106:753–61. [PubMed: 10995786]
31. Hoffmann I, Draetta G, Karsenti E. Activation of the phosphatase activity of human cdc25A by a cdk2-cyclin E dependent phosphorylation at the G_1/S transition. Embo J 1994;13:4302–10. [PubMed: 7523110]
32. Vigo E, Muller H, Prosperini E, Hateboer G, Cartwright P, Moroni MC, et al. CDC25A phosphatase is a target of E2F and is required for efficient E2F-induced S phase. Mol Cell Biol 1999;19:6379–95. [PubMed: 10454584]
33. Lundberg AS, Weinberg RA. Functional inactivation of the retinoblastoma protein requires sequential modification by at least two distinct cyclin-cdk complexes. Mol Cell Biol 1998;18:753–61. [PubMed: 9447971]
34. Youn CK, Cho HJ, Kim SH, Kim HB, Kim MH, Chang IY, et al. Bcl-2 expression suppresses mismatch repair activity through inhibition of E2F transcriptional activity. Nat Cell Biol 2005;7:137–47. [PubMed: 15619620]

NIH-PA Author Manuscript NIH-PA Author Manuscript NIH-PA Author Manuscript

35. Hall A. Rho GTPases and the control of cell behaviour. Biochem Soc Trans 2005;33:891–5. [PubMed: 16246005]
36. Olson MF, Ashworth A, Hall A. An essential role for Rho, Rac, and Cdc42 GTPases in cell cycle progression through G_1. Science 1995;269:1270–2. [PubMed: 7652575]
37. Schmidt A, Durgan J, Magalhaes A, Hall A. Rho GTPases regulate PRK2/PKN2 to control entry into mitosis and exit from cytokinesis. Embo J 2007;26:1624–36. [PubMed: 17332740]
38. Narumiya S, Oceguera-Yanez F, Yasuda S. A new look at Rho GTPases in cell cycle: role in kinetochore-microtubule attachment. Cell Cycle 2004;3:855–7. [PubMed: 15190208]
39. Philips A, Roux P, Coulon V, Bellanger JM, Vie A, Vignais ML, et al. Differential effect of Rac and Cdc42 on p38 kinase activity and cell cycle progression of nonadherent primary mouse fibroblasts. J Biol Chem 2000;275:5911–7. [PubMed: 10681583]
40. Molnar A, Theodoras AM, Zon LI, Kyriakis JM. Cdc42Hs, but not Rac1, inhibits serum-stimulated cell cycle progression at G_1/S through a mechanism requiring p38/RK. J Biol Chem 1997;272:13229–35. [PubMed: 9148940]
41. Lamb J, Ramaswamy S, Ford HL, Contreras B, Martinez RV, Kittrell FS, et al. A mechanism of cyclin D1 action encoded in the patterns of gene expression in human cancer. Cell 2003;114:323–34. [PubMed: 12914697]
42. Roy PG, Thompson AM. Cyclin D1 and breast cancer. Breast 2006;15:718–27. [PubMed: 16675218]
43. Li Z, Wang C, Prendergast GC, Pestell RG. Cyclin D1 functions in cell migration. Cell Cycle 2006;5:2440–2. [PubMed: 17106256]
44. Cox BD, Natarajan M, Stettner MR, Gladson CL. New concepts regarding focal adhesion kinase promotion of cell migration and proliferation. J Cell Biochem 2006;99:35–52. [PubMed: 16823799]
45. Danen EH, Sonneveld P, Sonnenberg A, Yamada KM. Dual stimulation of Ras/mitogen-activated protein kinase and RhoA by cell adhesion to fibronectin supports growth factor-stimulated cell cycle progression. J Cell Biol 2000;151:1413–22. [PubMed: 11134071]
46. Dean DC, Newby RF, Bourgeois S. Regulation of fibronectin biosynthesis by dexamethasone, transforming growth factor beta, and cAMP in human cell lines. J Cell Biol 1988;106:2159–70. [PubMed: 2454932]
47. Han EK, Ng SC, Arber N, Begemann M, Weinstein IB. Roles of cyclin D1 and related genes in growth inhibition, senescence and apoptosis. Apoptosis 1999;4:213–9. [PubMed: 14634283]
48. Pagano M, Theodoras AM, Tam SW, Draetta GF. Cyclin D1-mediated inhibition of repair and replicative DNA synthesis in human fibroblasts. Genes Dev 1994;8:1627–39. [PubMed: 7958844]
49. Miyashita T, Kitada S, Krajewski S, Horne WA, Delia D, Reed JC. Overexpression of the Bcl-2 protein increases the half-life of p21Bax. J Biol Chem 1995;270:26049–52. [PubMed: 7592801]
50. Alao JP. The regulation of cyclin D1 degradation: roles in cancer development and the potential for therapeutic invention. Mol Cancer 2007;6:24. [PubMed: 17407548]
51. Linette GP, Li Y, Roth K, Korsmeyer SJ. Cross talk between cell death and cell cycle progression: BCL-2 regulates NFAT-mediated activation. Proc Natl Acad Sci USA 1996;93:9545–52. [PubMed: 8790367]
52. Chen R, Valencia I, Zhong F, McColl KS, Roderick HL, Bootman MD, et al. Bcl-2 functionally interacts with inositol 1,4,5-trisphosphate receptors to regulate calcium release from the ER in response to inositol 1,4,5-trisphosphate. J Cell Biol 2004;166:193–203. [PubMed: 15263017]
53. Kuo TH, Kim HR, Zhu L, Yu Y, Lin HM, Tsang W. Modulation of endoplasmic reticulum calcium pump by Bcl-2. Oncogene 1998;17:1903–10. [PubMed: 9788433]
54. Papp S, Fadel MP, Kim H, McCulloch CA, Opas M. Calreticulin affects fibronectin-based cell-substratum adhesion via the regulation of c-Src activity. J Biol Chem 2007;282:16585–98. [PubMed: 17389592]
55. Chiou SK, Rao L, White E. Bcl-2 blocks p53-dependent apoptosis. Mol Cell Biol 1994;14:2556–63. [PubMed: 8139558]
56. Shen Y, Shenk T. Relief of p53-mediated transcriptional repression by the adenovirus E1B 19-kDa protein or the cellular Bcl-2 protein. Proc Natl Acad Sci USA 1994;91:8940–4. [PubMed: 8090749]
57. Kasof GM, Goyal L, White E. Btf, a novel death-promoting transcriptional repressor that interacts with Bcl-2-related proteins. Mol Cell Biol 1999;19:4390–404. [PubMed: 10330179]

NIH-PA Author Manuscript

NIH-PA Author Manuscript

NIH-PA Author Manuscript

58. Miyashita T, Mami U, Inoue T, Reed JC, Yamada M. Bcl-2 relieves the trans-repressive function of the glucocorticoid receptor and inhibits the activation of CPP32-like cysteine proteases. Biochem Biophys Res Commun 1997;233:781–7. [PubMed: 9168933]
59. Grimm S, Bauer MK, Baeuerle PA, Schulze-Osthoff K. Bcl-2 downregulates the activity of transcription factor NFkappaB induced upon apoptosis. J Cell Biol 1996;134:13–23. [PubMed: 8698809]
60. Fernando R, Foster JS, Bible A, Strom A, Pestell RG, Rao M, et al. Breast cancer cell proliferation is inhibited by BAD: regulation of cyclin D1. J Biol Chem 2007;282:28864–73. [PubMed: 17670745]
61. Yoshida K, Venkatesh L, Kuppuswamy M, Chinnadurai G. Adenovirus transforming 19-kD T antigen has an enhancer-dependent trans-activation function and relieves enhancer repression mediated by viral and cellular genes. Genes Dev 1987;1:645–58. [PubMed: 2962899]
62. See RH, Shi Y. Adenovirus E1B 19,000-molecular-weight protein activates c-Jun N-terminal kinase and c-Jun-mediated transcription. Mol Cell Biol 1998;18:4012–22. [PubMed: 9632786]
63. Bild AH, Yao G, Chang JT, Wang Q, Potti A, Chasse D, et al. Oncogenic pathway signatures in human cancers as a guide to targeted therapies. Nature 2006;439:353–7. [PubMed: 16273092]
64. Zinkel S, Gross A, Yang E. BCL2 family in DNA damage and cell cycle control. Cell Death Differ 2006;13:1351–9. [PubMed: 16763616]
65. Summers K, da Silva J, Farwell M. Intragenomic conflict and cancer. Med Hypotheses 2002;59:170–9. [PubMed: 12208205]
66. Nunez G, London L, Hockenbery D, Alexander M, McKearn JP, Korsmeyer SJ. Deregulated Bcl-2 gene expression selectively prolongs survival of growth factor-deprived hemopoietic cell lines. J Immunol 1990;144:3602–10. [PubMed: 2184193]
67. Protocols. 2005. http://www.grc.nia.nih.gov/branches/rrb/dna/index/protocols.htmhttp://www.grc.nia.nih.gov/branches/rrb/dna/index/protocols.htm
68. McGinnis S, Madden TL. BLAST: at the core of a powerful and diverse set of sequence analysis tools. Nucleic Acids Res 2004;32:20–5.
69. Pattyn F, Robbrecht P, De Paepe A, Speleman F, Vandesompele J. RTPrimerDB: the real-time PCR primer and probe database, major update 2006. Nucleic Acids Res 2006;34:684–8.
70. Zuker M, Stiegler P. Optimal computer folding of large RNA sequences using thermodynamics and auxiliary information. Nucleic Acids Res 1981;9:133–48. [PubMed: 6163133]
71. Skaletsky, SRaHJ. Primer3 on the WWW for general user and biologist programmers. Humana Press; Totowa, NJ: 2000.
72. Livak KJ, Schmittgen TD. Analysis of relative gene expression data using real-time quantitative PCR and the 2(-Delta Delta C(T)) Method. Methods 2001;25:402–8. [PubMed: 11846609]
73. Bradford MM. A rapid and sensitive method for the quantitation of microgram quantities of protein utilizing the principle of protein-dye binding. Anal Biochem 1976;72:248–54. [PubMed: 942051]

NIH-PA Author Manuscript

NIH-PA Author Manuscript

NIH-PA Author Manuscript

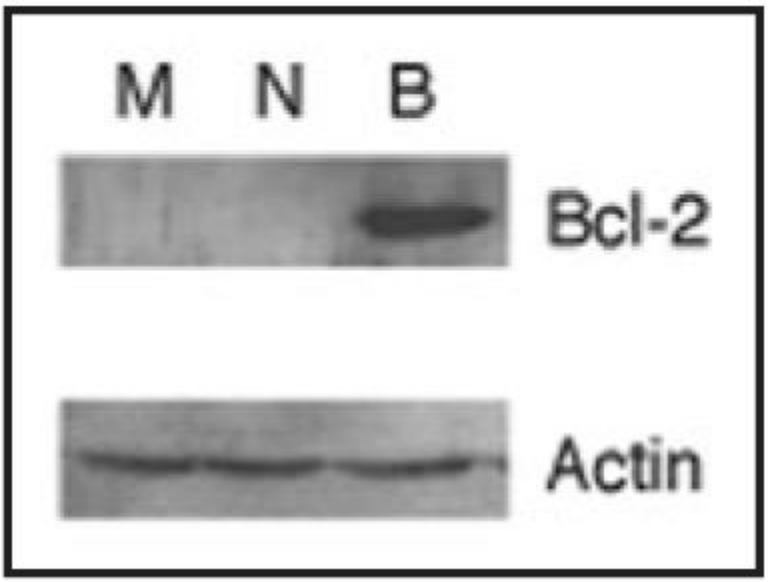

Figure 1.

Western blot analysis of MCF10A (M), MCF10A/Neo (N) and MCF10A/Bcl-2 (B), with an antibody to Bcl-2. Lysates were prepared from exponentially proliferating cells. Protein (30 μg) was loaded onto a 12% SDS PAGE gel and subjected to immunoblot analysis. β actin antibody was used as a loading control.

NIH-PA Author Manuscript

NIH-PA Author Manuscript

NIH-PA Author Manuscript

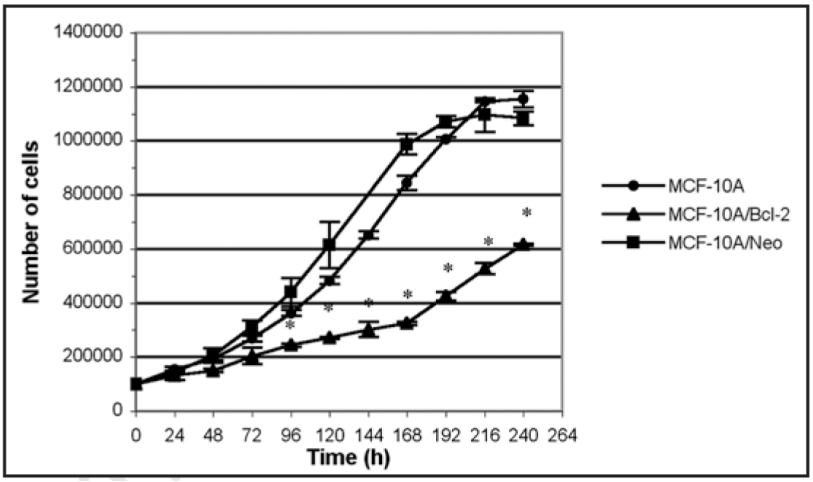

Figure 2.

Graph depicting the growth curves for MCF10A, MCF10A/Neo, and MCF10A/Bcl-2. Each cell line was plated at 100,000 cells per 35 mm dish and counted by trypan blue exclusion every day for 10 days. Points represent means, error bars represent standard error of three independent experiments.

NIH-PA Author Manuscript

NIH-PA Author Manuscript

NIH-PA Author Manuscript

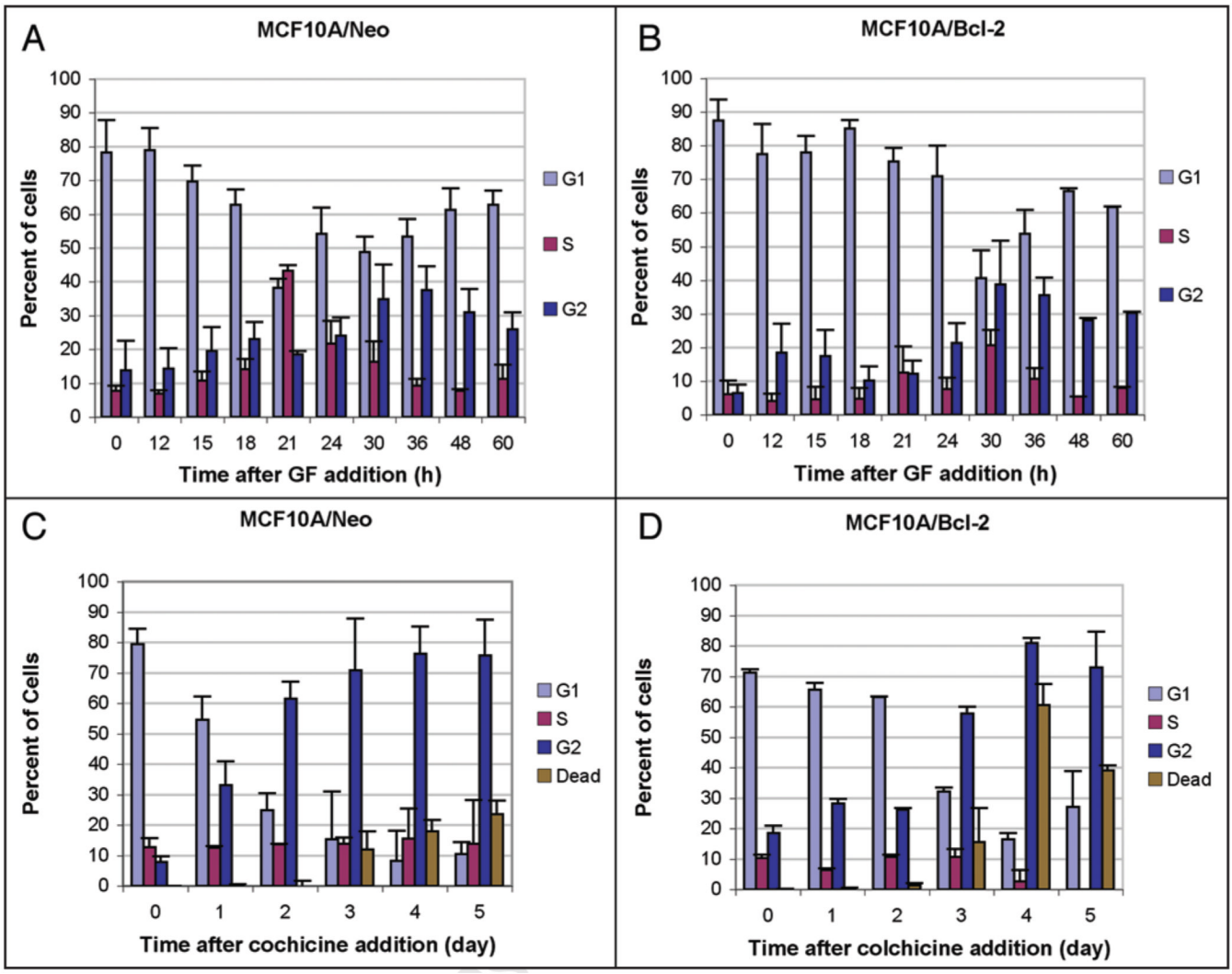

Figure 3.

Analysis of the cell cycle of MCF10A/Neo (A) and MCF10A/Bcl-2 cells (B) by growth factor withdrawal (GF) and MCF10A/Neo (C) and MCF10A/Bcl-2 (D) cells by colchicine treatment. For (A and B), cells were incubated without GF for five days and then GF were added, and cells were grown for an additional 60 h. For (C and D), cells were treated with 100 nM colchicine for five days. At each time point, cells were fixed in ethanol and stored at −20°, then were treated with RNAse, stained with PI, and analyzed by flow cytometry with ModFit software. Bars represent means, error bars represent the standard error of three independent experiments carried out in duplicate.

NIH-PA Author Manuscript

NIH-PA Author Manuscript

NIH-PA Author Manuscript

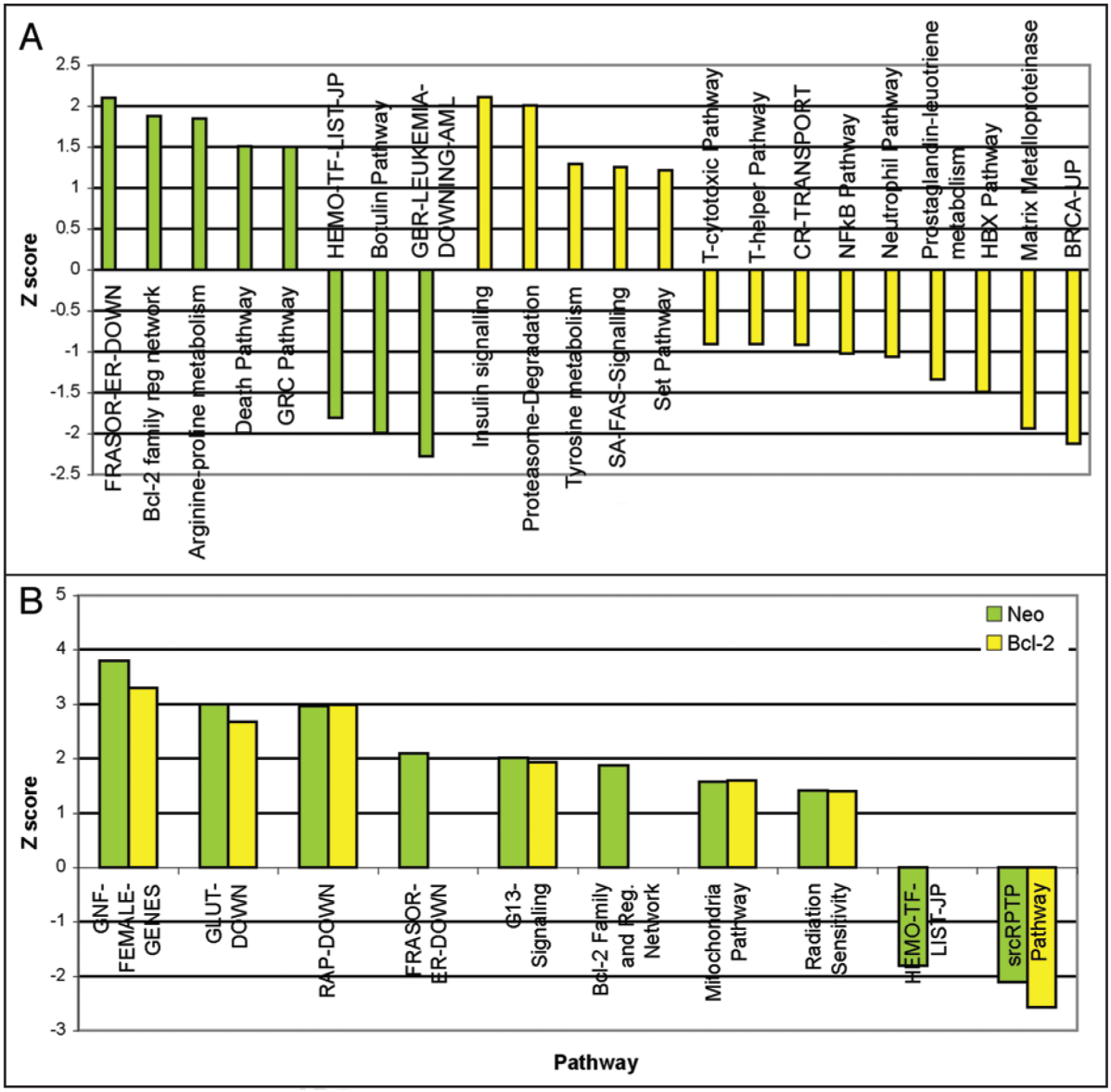

Figure 4.

(A) PAGE bar graph representing pathways significantly different between MCF10A/Neo (green) and MCF10A/Bcl-2 (gold) cell lines and the pathway corresponding Z score. (B) Bar graph representing ten gene sets identified by PAGE that contained one or more target genes. Three of the gene sets shown were identified as being significantly different between the two cell lines: Frasor ER Down, Bcl-2 Family and Regulatory Network, and Hemo TF List JP. These pathways are named according to their gene complement.[25] See text for details.

NIH-PA Author Manuscript

NIH-PA Author Manuscript

NIH-PA Author Manuscript

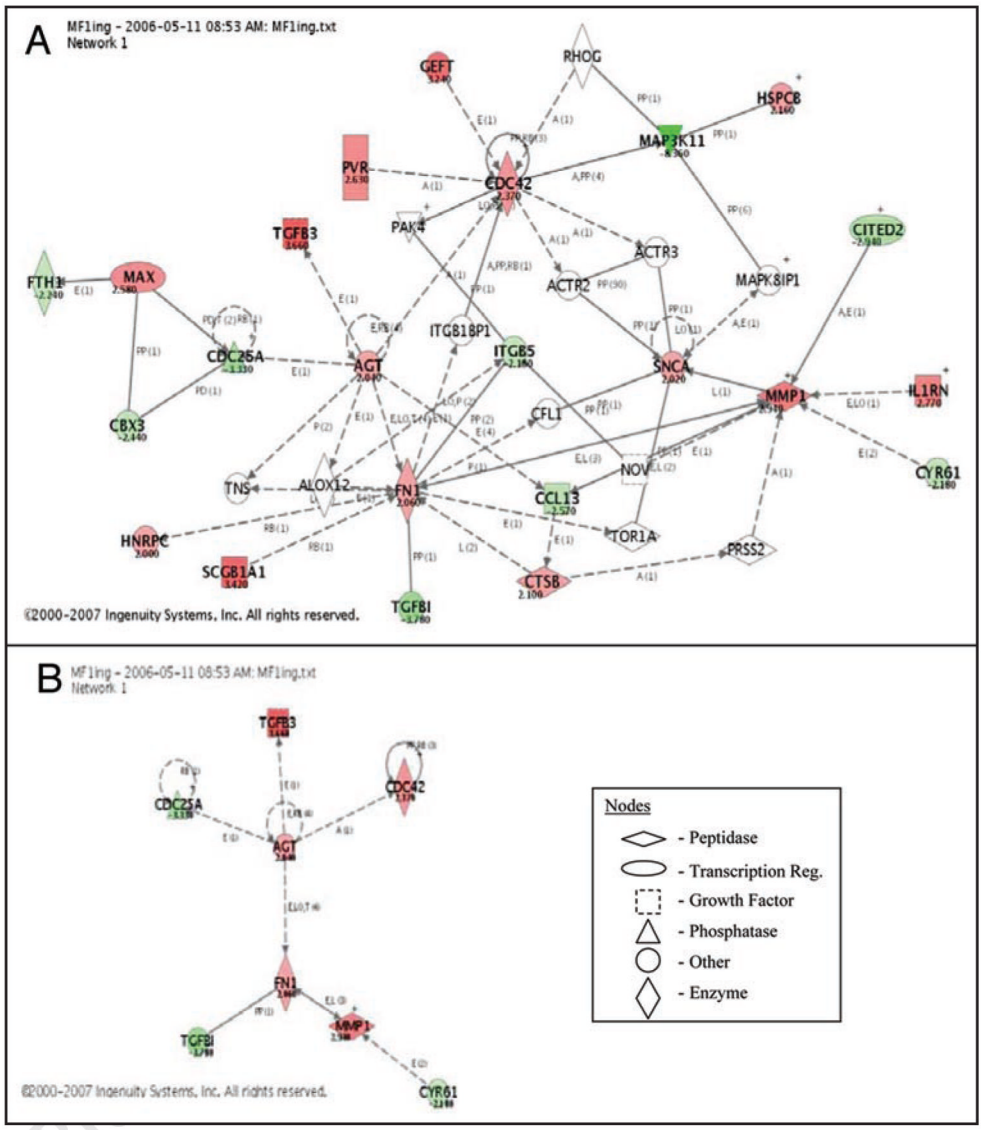

Figure 5.

(A) Ingenuity pathway analysis (IPA) network representation of the most highly rated network. The genes that are shaded were determined to be significant from the statistical analysis. The intensity of the shading shows to what degree each gene was up or downregulated. The Z ratio is also displayed under each shaded gene. The genes shaded red are upregulated and those that are green are downregulated. A solid line represents a direct interaction between the two gene products and a dotted line means there is an indirect interaction. (B) Network showing only the interactions of the nine target genes.

NIH-PA Author Manuscript

NIH-PA Author Manuscript

NIH-PA Author Manuscript

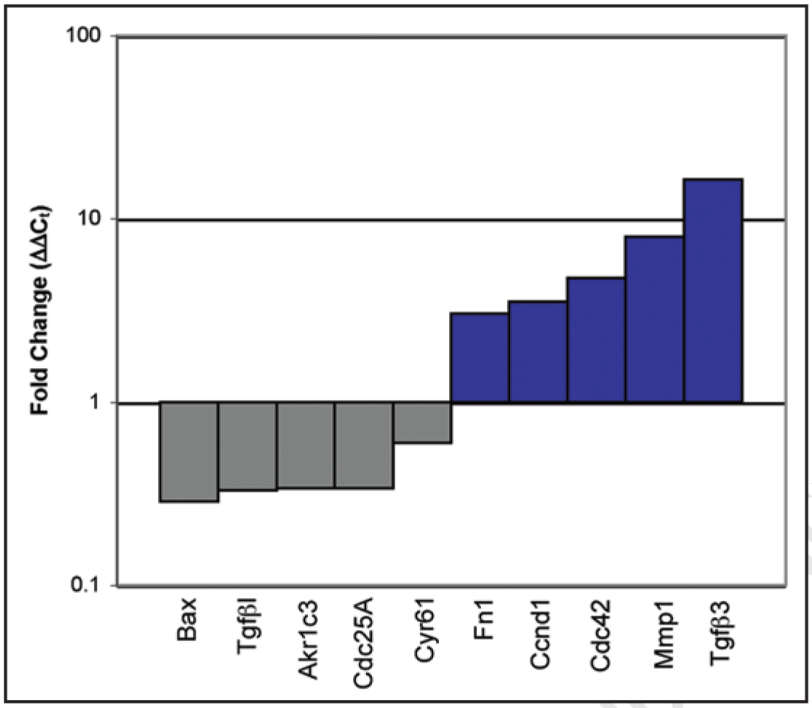

Figure 6.

Comparison of the fold change values ($\Delta\Delta$ C_t) obtained from qRTPCR analysis for each gene in the network shown in Figure 5B, plus Bax. Genes that were upregulated according to the microarray analysis (blue) showed a significant increase in expression and genes that were down-regulated according to the microarray showed a significant decrease in expression (grey).

NIH-PA Author Manuscript

NIH-PA Author Manuscript

NIH-PA Author Manuscript

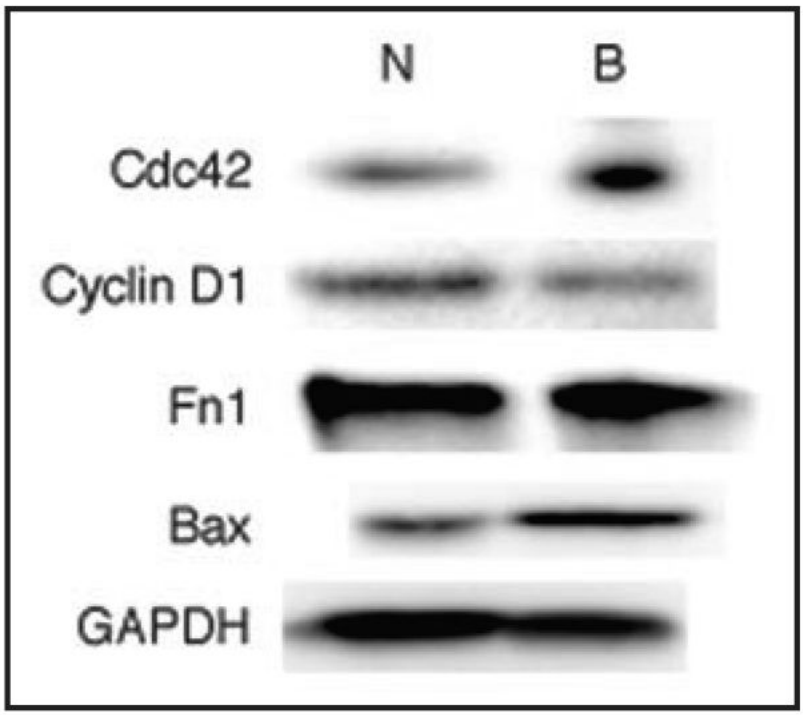

Figure 7.
Western blot of MCF10A/Neo (N) and MCF10A/Bcl-2 (B) cell lines. Protein (50 μg) was subjected to SDS-PAGE followed by immuno-blotting analysis with corresponding antibodies. GAPDH was used as a loading control.

NIH-PA Author Manuscript NIH-PA Author Manuscript NIH-PA Author Manuscript

Table 1

Genes from the microarray found in the most significant IPA network

Gene name	Gene symbol	GeneID	Z-ratio	Confirmed by qRT-PCR	Fold increase or decrease
Transforming growth factor beta-induced	*TGFβI*	7045	−3.78	Yes	0.29
Aldo-keto reductase family 1, member C3	*AKR1C3*	8644	−2.59	Yes	0.34
Cell Division Cycle 25 homolog A	*CDC25A*	993	−3.33	Yes	0.34
Cystein-rich, angiogenic inducer	*CYR61*	3491	−2.18	Yes	0.59
Fibronectin 1	*FN1*	2335	3.03	Yes	3.03
Cyclin D1	*CCND1*	595	1.69	Yes	3.54
Cell Division Cycle 42	*CDC42*	998	2.37	Yes	4.75
Matrix metalloproteinase 1	*MMP1*	4312	2.94	Yes	7.21
Transforming growth factor beta-3	*TGFβ3*	7043	3.66	Yes	10.56

NIH-PA Author Manuscript

NIH-PA Author Manuscript

NIH-PA Author Manuscript

Table 2

Genes amplified by qRT-PCR and their primers

Gene symbol	GenBank accession number	Amplicon	Primer sequence
BCL2	NM_000633	127 bp	For 5′-CCTGTGGATGACTGAGTACC-3′ Rev 5′-GAGACAGCCAGGAGAAATCA-3′
BAX	NM_138761	115 bp	For 5′-TTTGCTTCAGGGTTTCATC-3′ Rev 5′-CGTCCCAAAGTAGGAGAGGA-3′
CDC25A	NM_001789	150 bp	For 5′-GCCTGTCACCAACCTGAC-3′ Rev 5′-CCAGGAGAATCTAGACAGAAACC-3′
CDC42	NM_001791	116 bp	For 5′-GCTGTCAAGTATGTGGAGTG-3′ Rev 5′-ACACACCTGCGGCTCTTCTT-3′
CCND1	NM_053056	75 bp	For 5′- GCTCCTGGTGAACAAGCTCAA-3′ Rev 5′-TTGGAGAGGAAGTGTTCAATGAA-3′
CYR61	NM_001554	100 bp	For 5′-ACTTCATGGTCCCAGTGCTC-3′ Rev 5′-AAATCCGGGTTTCTTTCACA-3′
AKR1C3	NM_003739	85 bp	For 5′-GTAAGGATGCAGGATTGG-3′ Rev 5′-AGTCCTGGCTTGTTGAGG-3′
FN1	NM_212482	92 bp	For 5′-TGTCTTGGTAATGGAAAAGG-3′ Rev 5′-TCTCCGACCACATAGGAAG-3′
MMP1	NM_002421	72 bp	For 5′-GGGAGATCATCGGGACAACTC-3′ Rev 5′-GGGCCTGGTTGAAAAGCAT-3′
TGFβ3	NM_003239	82 bp	For 5′-ATGGAAATCAAATTCAAAGG-3′ Rev 5′-ATTAGATGAGGGTTGTGGTG-3′
TGFβI	NM_000358	115 bp	For 5′-GCTGTCCTGGATATGAAAAG-3′ Rev 5′-GTGTACAGCTGAGTGGTGGT-3′